Pharmaceutical Biology

ISSN: 1388-0209 (Print) 1744-5116 (Online) Journal homepage: http://www.tandfonline.com/loi/iphb20

Anti-proliferative and antibacterial in vitro evaluation of the polyurethane nanostructures incorporating pentacyclic triterpenes

Camelia Oprean, Csilla Zambori, Florin Borcan, Codruta Soica, Istvan Zupko, Renata Minorics, Florina Bojin, Rita Ambrus, Delia Muntean, Corina Danciu, Iulia Andreea Pinzaru, Cristina Dehelean, Virgil Paunescu & Gabriela Tanasie

To cite this article: Camelia Oprean, Csilla Zambori, Florin Borcan, Codruta Soica, Istvan Zupko, Renata Minorics, Florina Bojin, Rita Ambrus, Delia Muntean, Corina Danciu, Iulia Andreea Pinzaru, Cristina Dehelean, Virgil Paunescu & Gabriela Tanasie (2016): Anti-proliferative and antibacterial in vitro evaluation of the polyurethane nanostructures incorporating pentacyclic triterpenes, Pharmaceutical Biology

To link to this article: http://dx.doi.org/10.1080/13880209.2016.1180538

Published online: 09 May 2016.

PHARMACEUTICAL BIOLOGY, 2016
http://dx.doi.org/10.1080/13880209.2016.1180538

Taylor & Francis
Taylor & Francis Group

RESEARCH ARTICLE

Anti-proliferative and antibacterial *in vitro* evaluation of the polyurethane nanostructures incorporating pentacyclic triterpenes

Camelia Oprean[a], Csilla Zambori[b], Florin Borcan[a], Codruta Soica[a], Istvan Zupko[c], Renata Minorics[c], Florina Bojin[b], Rita Ambrus[d], Delia Muntean[b], Corina Danciu[a], Iulia Andreea Pinzaru[a], Cristina Dehelean[a], Virgil Paunescu[b] and Gabriela Tanasie[b]

[a]Faculty of Pharmacy, University of Medicine and Pharmacy "Victor Babeş", Timişoara, România; [b]Faculty of Medicine, University of Medicine and Pharmacy "Victor Babeş", Timişoara, România; [c]Department of Pharmacodynamics and Biopharmacy, University of Szeged, Szeged, Hungary; [d]Department of Pharmaceutical Technology, University of Szeged, Szeged, Hungary

ABSTRACT

Context: Oleanolic and ursolic acids are antitumor and antibacterial agents which are extensively studied. Their major disadvantage is the poor water solubility which limits their applications.

Objectives: Oleanolic and ursolic acid were encapsulated into polyurethane nanostructures that act as drug carriers. In order to evaluate the effectiveness of the particles, anti-microbial and anti-proliferative activity compared to un-encapsulated active compounds was tested.

Materials and methods: Using an interfacial polycondensation technique, combined with spontaneous emulsification, structures with nanoscale dimensions were obtained. Scanning electron microscopy, differential scanning calorimetry and X-ray assays confirmed the encapsulation process. Concentrations of 10 and 30 μM particles and un-encapsulated compounds were tested by MTT viability assay for several breast cancer lines, with an exposure time of 72 h. For the antibacterial studies, the dilution method with MIC determination was used.

Results: Ursolic acid had an excellent inhibitory effect with IC_{50} value of 2.47, 1.20, 1.26 and 1.34 μM on MCF7, T47D, MDA-MB-231 and MDA-MB-361, respectively. Oleanolic acid did not show anti-proliferative activity. The pure compounds showed their antibacterial activity only against *Bacillus* species and *Candida albicans,* but MIC values were too high to be considered efficient antimicrobial agents (2280 and 4570 μg mL^{-1}, respectively). Polyurethane nanoparticles which incorporated the agents did not show any biological activity.

Discussion and conclusion: Although the active compounds did not fully exert their anti-proliferative activity following encapsulation inside polymeric nanoparticles, *in vivo* evaluation is needed in order to obtain an exhaustive conclusion, as the active compounds could be released as a result of metabolic activity.

ARTICLE HISTORY
Received 23 March 2015
Revised 12 January 2016
Accepted 14 April 2016
Published online 5 May 2016

KEYWORDS
Antitumor; breast cancer; minimal inhibitory concentration; oleanolic acid; ursolic acid

Introduction

Breast cancer is one of the most common cancers worldwide, being the second leading cause of cancer related death, after lung cancer, in the USA. Further, it is the most common women malignancies (Wang et al. 2012). In spite of major research, efforts in developing new therapeutic modalities, effective cure of locally advanced or metastatic cancers remains an unmet goal in oncology. Also, many chemotherapy and targeted drugs, and combinations of the two, have substantial systemic toxicity which often limits their administration (Workman 2001). Much attention is now devoted to cancer prevention and early detection and to the development of less toxic treatments. In this context, new classes of compounds are being explored, in particular, plant-derived molecules, including pentacyclic triterpenes. Triterpenes are compounds widely-spread in plants and an integral part of commonly consumed foods. Pentacyclic triterpenes consist of a 30-carbon skeleton formed by the cyclization of squalene (Gayathri et al. 2010; George et al. 2012) exhibiting mainly anti-proliferative properties (Dehelean et al. 2011, 2012). Oleanolic acid (OA) (3β-hydroxy-olean-12-en-28-oic acid) and its isomer ursolic acid (UA) (3β-hydroxy-urs-12-en-28-oic acid) are triterpenoids (Feng et al. 2009) with pharmacological activity ranging from antitumor, antiviral, anti-inflammatory, hepatoprotective, antidiabetic and gastro-protective activities (Sun et al. 2006; Prasad et al. 2012). Although antitumor activities of OA and UA were reported in cancers (breast, liver, prostate), melanoma, leukemia and lymphomas, both *in vitro* and *in vivo* (Sun et al. 2006; Yim et al. 2006; Zhang et al. 2007), their mechanisms of action remain largely elusive.

Recently, these pentacyclic triterpenes have been studied for their antibacterial activity, as well as for their potential to enhance the susceptibility of bacteria to antibiotics (Kurek et al. 2012; do Nascimento et al. 2013), bacterial resistance remains a serious challenge of the 21st century (Fontanay et al. 2008; Mokoka et al. 2013). UA and OA have also showed antimicrobial and antifungal activity, in some cases even on methicillin- or vancomycin-resistant strains (Horiuchi et al. 2007; Kim et al. 2012).

Bioavailability of these compounds is limited by low water solubility leading to low efficiency, which is worsened by its non-specific distribution in the body (Lopes et al. 2013; Zhang et al. 2013). In the last decade, nanotechnology has provided possible

CONTACT Csilla Zambori csillaza@yahoo.com Faculty of Medicine, University of Medicine and Pharmacy "Victor Babeş", Timişoara, România

solutions to the bioavailability limitations of active substances, limitations which influence the effectiveness of the active compounds in therapy (Lopes et al. 2013).

The aim of this study was the synthesis of a polyurethane drug delivery system with oleanolic and ursolic acids incorporated as active drugs and the determination of their anti-proliferative activity on breast cancer cell lines as well as their antibacterial activity against several bacterial strains.

Materials and methods

Substances

UA and OA of analytical purity were purchased from Fluka (Sigma Aldrich, Steinheim, Germany). The chemicals were purchased as follows: ethylene glycol (EG) from Lach-Ners.r.o. (Czech R.), 1,4-butanediol (BD) from Carl Roth GmbH (Germany). Polyethylene glycol M = 200 (PEG), the solvent (acetone), isophorone diisocyanate (IPDI) and surfactants (Span®85 and Tween®20) were purchased from Merck (Germany). All substances and reagents were used as received.

Synthesis of polyurethane drug delivery system

Polyurethane particles were synthesized as described in literature (Bouchemal et al. 2004), using a multi-step procedure based on the interfacial polycondensation technique combined with spontaneous emulsification. The organic phase (1.5 mL IPDI, 1.5 mL Span®85, mixed with 15 mL acetone and heated at 30 °C) was injected into the aqueous phase (0.8 mL EG, 0.8 mL BD, 0.3 mL PEG and 1.5 mL Tween®20 mixed with 15 mL distilled water and heated at 30 °C). The injection of organic phase into the aqueous phase was made under magnetic stirring (500 rpm) and heated (40 °C) for 4 h in order to ensure the completion of the chemical reaction. The products were repeatedly washed with a mixture acetone/water (1:2, v/v). After synthesis, the obtained particles were maintained as thin layers (around 3 mm thickness) in Petri dishes at 80 °C in an oven for 12 h, for acetone and water removal. Oleanolic and ursolic acids were separately added (in organic phase) in two experiments while in the third one empty polymeric nanoparticles were used as control.

Nanoparticle size distribution

The size distribution of the obtained polyurethane nanoparticles was measured using a particle size analyzer (Vasco from Cordouan Tech., Pessac, France). Solutions of 1:100 (w/w) in ethanol were prepared. The parameters used were as follows: 25 °C temperature, 190 channels, 80% laser power, 18 µs time interval, continuous acquisition mode and Log-normal dispersion. Three measurements were done for each sample and an average value was considered.

Differential scanning calorimetry (DSC)

Heating behavior was assessed by differential scanning calorimetry (DSC), measuring the heat energy that occurs with phase changes in the sample when subjected to temperature change. Measurements were made using a Mettler Toledo STAR Thermal Analysis System, DSC 821 (Mettler Inc., Schwerzenbach, Switzerland). Argon was used as carrier gas at a flow rate of 10 L h^{-1} during the DSC investigation. Approximately 2–5 mg of ursolic acid, oleanolic acid and their nanoparticles were examined in a temperature range from 25 to 350 °C with a heating rate of 5 °C/min.

X-ray diffraction

A Philips PW 1710 diffractometer (PW 1930 generator, PW 1820 goniometer, Angstrom Advanced Inc., Braintree, MA) was used to obtain the X-ray-diffraction patterns. The tube anode was Cu with $K\alpha = 1.54242$ Å. The pattern was collected with a tube voltage of 50 kV and 40 mA of tube current in step scan mode (step size 0.035, counting time 1 s per step).

Scanning electron microscopy (SEM) assay

The shape and crystal morphology of the particles were measured using scanning electron microscopy (SEM) (Hitachi S4700, Hitachi Scientific Ltd., Hitachi, Japan) as described in the literature (Soica et al. 2012). Electric conductivity on the surface of the samples was induced by a sputter coating apparatus (Bio-Rad SC 502, VG Microtech, Uckfield, UK). The air pressure was 1.3–13.0 mPa. The samples were fixed onto a metallic stub with double-sided conductive tape (diameter 12 mm, Oxon, Oxford Instruments, Abington, UK). Images were taken in secondary electron image mode at 10 kV acceleration voltages.

Particle cellular uptake studies

Nanoparticle internalization studies were performed using a fluorescent marker, as described in the literature (Zhang et al. 2013). Coumarin-6 loaded nanoparticles (12.5 µg mL^{-1}) were prepared using the interfacial polycondensation technique combined with spontaneous emulsification as described in the above section. 5×10^4 MCF-7 cells were seeded into 24-well plates and incubated overnight in 5% CO_2 atmosphere at 37 °C. After 24 h, the medium was replaced with a new medium containing coumarin-6 loaded nanoparticles and cells were incubated for 24 and 48 h, respectively. After the incubation period, the medium was removed and cells were rinsed with a new medium. Fluorescence microscopy (Nikon Eclipse TE300, Amstelveen, The Netherlands) with FITC/DAPI/Hoechst filters was used to observe the efficiency of coumarin-6 loaded nanoparticles internalization in cells. After 48 h of exposure, cell nuclei were counterstained with Hoechst dye (5 min incubation in the dark, followed by supernatant removal and microscope visualization).

In vitro *antibacterial activity*

Oleanolic acid, ursolic acid and their polyurethane structures were tested for their antimicrobial activity against six bacterial strains: *Staphylococcus aureus* (ATCC25923), *Escherichia coli* (ATCC25922), *Pseudomonas aeruginosa* (ATCC27853), *Salmonella enteritidis* (D) (ATCC 13076), *Bacillus subtilis* (6633), *Bacillus cereus* (14579); and *Candida albicans* (ATCC10231) by the dilution method with MIC (minimal inhibitory concentration) determination. All the bacterial strains used were prepared from 24 h old cultures. Suspensions were adjusted to a McFarland's standard of 0.5 (a final bacterial concentration of $1–2 \times 10^8$ CFU mL^{-1}). The final dilution was 1:200 bacteria in Muller-Hinton broth (Sanimed, Romania, Bucharest), which was incubated at 37 °C. This resulted in approximately 5×10^5 CFU mL^{-1}. In glass test tubes, a 200 µL bacterial suspension was

distributed to 200 µL of test medium containing the tested substances. These tubes were incubated for 18 h at 37 °C. The initial solutions of ursolic and oleanolic acids and their nanoparticles were obtained by dissolving the substances in 1 mL of dimethyl sulfoxide (DMSO) to obtain an initial concentration of 4.56 mg mL^{-1}. From this concentration, serial dilutions were made in distilled water in order to reach final concentrations in the range of 290–4570 µg mL^{-1}. The minimum concentration of the compound which inhibited the visible growth of the tested microorganism (MIC) was recorded. Since the stock solutions were prepared in DMSO, 20 µL of the solvent were introduced in a tube with 200 µL bacterial suspension and 180 µL nutrient medium, being used as negative control. As positive control for antimicrobial activity and *Candida albicans,* gentamicin and fluconazole were used. Triplicate tests were performed for all samples.

Cell culturing and anti-proliferative assay

Anti-proliferative assays were performed as described in literature (Soica et al. 2014). Four human breast cancer cell lines (MCF7, MDA-MB-231, MDA-MB-361 and T47D) were purchased from European Collection of Cell Cultures (Salisbury, UK). All the chemicals used for cell culturing, unless otherwise specified, were purchased from Sigma-Aldrich Ltd. (Budapest, Hungary). Cells were grown in minimal essential medium supplemented with 10% fetal bovine serum (FBS), 1% non-essential amino-acids and an antibiotic-antimycotic mixture in a humidified atmosphere of 5% CO_2 at 37 °C. 5000 cells/well were seeded onto 96-well plates and allowed to attach overnight. After 24 h, the medium containing the tested compounds was added and cells were incubated for 72 h. The tested concentrations were 10 and 30 µM. After the incubation time, when active substances exerted their action, viability was determined by the addition of 20 µL of [3-(4, 5-dimethylthiazol-2-yl)-2,5-diphenyltetrazolium bromide] solution (5 mg mL^{-1}) (Mosmann 1983). The precipitated formazan crystals were solubilized in DMSO and the absorbance was read with an ELISA reader at 545 nm. Cisplatin, a clinically utilized anticancer agent, was used as positive control on the cell lines. It exerted growth inhibition values of 66.9% and 96.8% (MCF7), 51.0% and 57.9% (T47D), 20.8% and 71.7% (MDA-MB-231), 67.5% and 87.7% (MDA-MB-361) at 10 and 30 µM, respectively.

In order to establish the IC_{50} values for ursolic acid, concentrations between 0.3 and 10 µM were tested.

Statistical analyses (One-Way ANOVA followed by Newman-Keuls post test) and calculations were performed by means of GraphPad Prism 4.0 (GraphPad Software; San Diego, CA, USA). All measurements were performed in triplicate and data were presented as mean ± standard deviation.

Results

Nanoparticles size distribution

Polyurethane nanoparticles containing the tested compounds were synthesized by using the interfacial polyaddition procedure combined with spontaneous emulsification. Figure 1 presents the results of the particle size distribution for the polyurethane nanoparticles incorporating OA (OA + PU), polyurethane nanoparticles incorporating UA (UA + PU) and empty polyurethane nanoparticles (PU). Nanoparticles size distributions were as follows: for OA + PU Dv50: 48.99 nm and Dv 90: 77.65 nm; for UA + PU Dv50: 9.77 nm and Dv90: 26.92 nm; for PU Dv 50: 18.63 nm and Dv90: 371.63 nm. For PU containing OA and UA samples only one particle population was obtained, which indicates that homogeneous samples were prepared. For PU sample, a second population was observed, which could be the result of nanoparticle agglomeration (Bouchemal et al. 2004). Several benefits of nanoparticles were described by Bouchemal et al. (2004), one of them being the enormous surface area which makes them suitable for pharmaceutical applications such as lipophilic encapsulated drugs for homogeneous release.

Scanning electron microscopy (SEM) assay

The morphology of the active substances of the polyurethane used for encapsulation and of the encapsulated compounds was obtained by SEM. The results are shown in Figure 2. The crystalline structures of ursolic acid (Figure 2(c)) and the amorphous structure of oleanolic acid (Figure 2(a)) can be noticed. Figures 2(b) and (d) exhibit a film, similar to Figure 2(e) (empty polyurethanic nanostructures), which leads us to the conclusion that the encapsulation process took place.

Differential scanning calorimetry (DSC)

Thermal behaviors of OA (a), PUs (b) and OA + PU (c) are depicted in Figure 3.1. In case of pure OA, loss of water is indicated by the endothermic peak at 117.29 °C. The melting point for OA is around 315 °C (Liu & Wang, 2007) and it was not observed within the temperature range of this study (25–300 °C). For the PU, no peak was observed in the range of study. The OA + PU revealed a similar curve as the empty structures, indicating the encapsulation of the active substance. Encapsulation of OA into the polyurethane vehicle does not change the melting point of the pure OA (no peak was observed under 300 °C).

Thermal behaviors of pure UA, UA + PU and PU are depicted in Figure 3.2. For UA, an endothermic peak was observed at 280.63 °C, indicating the melting point of the compound. The curves for PU and UA + PU display a similar profile. Moreover, these nanoparticles showed a heating behavior quite similar to the one presented in Figure 3.1, for the OA + PU. Altogether, data could lead to the conclusion that the encapsulation process of the active substances took place.

X-ray diffraction

Used to characterize changes in the crystalline structure of compounds after molecular interactions (Soica et al. 2014), X-ray diffraction analysis was used to assess the crystalline structure of UA (Figure 4.2(a)) and OA (Figure 4.1(a)). As shown in Figure 4.1a and 4.2a, crystalline compounds are characterized by sharp peaks, UA displaying a higher degree of crystallinity than OA. For the PU (Figure 4.1(b); 4.2(b)) and for the OA + PU (Figure 4.1(c)) and UA + PU (Figure 4.2(c)), the X-ray profile exhibits indistinguishable peaks, revealing the amorphous nature of the compounds. These changes in the crystalline state of the substances also act as indicators of the encapsulation process.

Particle cellular uptake studies

Figure 5 shows the microscopic images of MCF-7 cells treated with coumarin-6 loaded nanoparticles after 24 h (a) and 48 h (b) of incubation. As shown in Figure 5, nanoparticles uptake in the cells was a time-dependent process. At the 24 h exposure

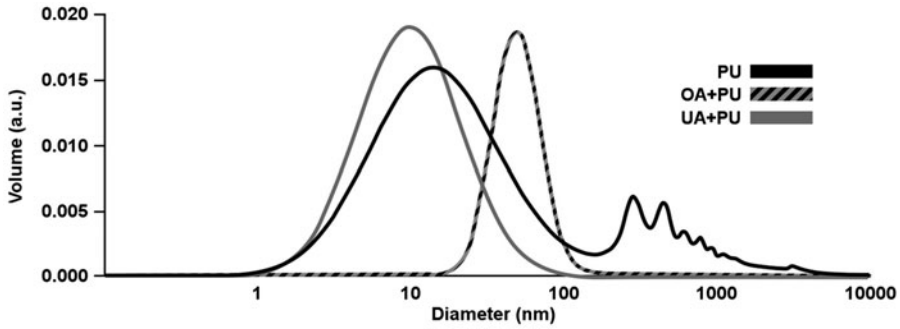

Figure 1. Distribution of polyurethane structures for: polyurethane nanoparticles containing oleanolic acid (OA + PU), polyurethane nanoparticles containing ursolic acid (UA + PU) and empty polyurethane nanoparticles (PU). Parameters used were: 25 °C, 190 channels, 80% laser power, 18 μs time interval, continuous acquisition mode and Log-normal dispersion.

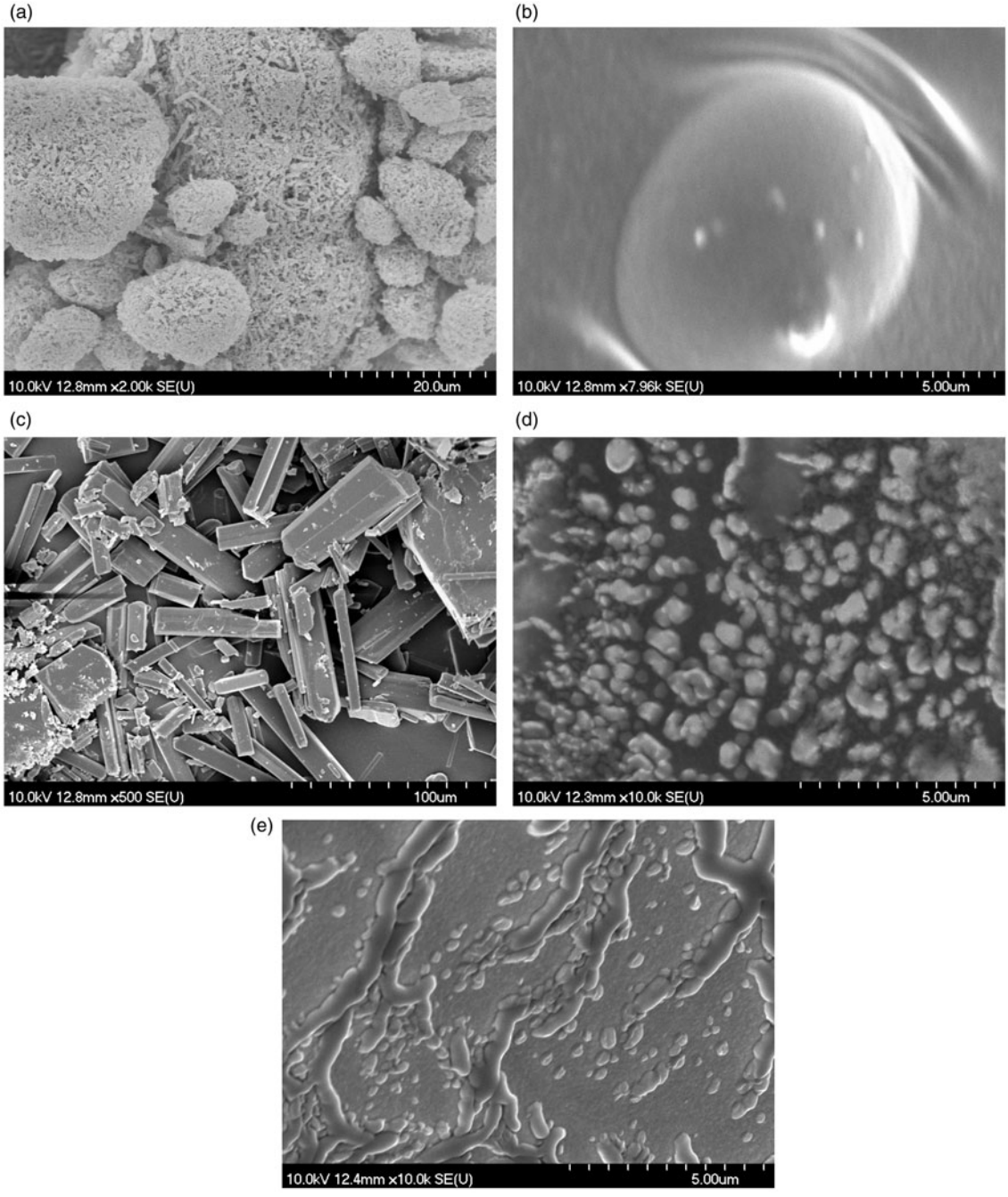

Figure 2. Scanning electron microscopy (SEM) pictures for: (a) oleanolic acid (OA); (b) polyurethane nanostructures containing oleanolic acid (OA + PU); (c) ursolic acid (UA); (d) polyurethane nanostructures containing ursolic acid (UA + PU); (e) empty polyurethane nanostructures (PU).

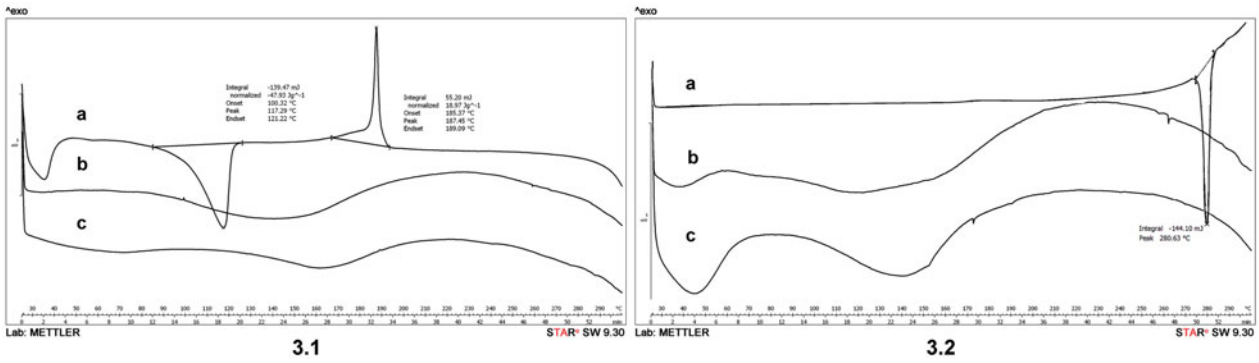

Figure 3. Differential scanning calorimetry (DSC) curves of: (a) oleanolic acid (OA) (3.1) and ursolic acid (UA) (3.2), (b) empty polyurethane nanostructures (PU) (3.1; 3.2), (c) polyurethane nanostructures containing oleanolic acid (OA + PU) (3.1) and ursolic acid (UA + PU) (3.2). Argon was used as carrier gas, the temperature range was between 25 up and 300 °C, and the heating rate was 5 °C min^{-1}, while the sample weight was 2–5 mg.

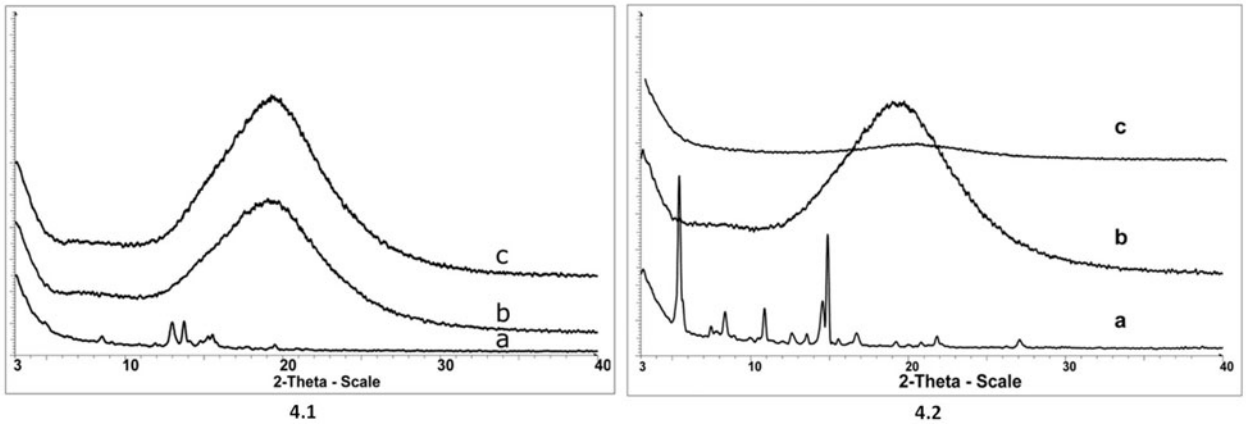

Figure 4. X-ray diffractograms of: (a) oleanolic acid (OA) (4.1) and ursolic acid (UA) (4.2), (b) empty polyurethane nanostructures (PU) (4.1; 4.2), (c) polyurethane nanostructures containing oleanolic acid (OA + PU) (4.1) and ursolic acid (UA) (4.2). The measurements were conducted with a 50 kV tube voltage and tube current of 40 mA in step scan mode (step size 0.035, counting time 1 s per step).

timepoint, the coumarin-6 loaded nanoparticles were localized mostly onto the cellular membrane (Figure 5a). After 48 h of exposure, nanoparticles were localized around the cells nuclei and inside the cytoplasm (Figure 5b). As reported by Zhang et al. (2013) and others (Rosen & Abribat 2005), cellular uptake of nanoparticles is an important factor which influences the efficiency of therapeutic effects.

Anti-proliferative activity

Figures 6 and 7 show the growth inhibition percent of the breast cancer cell lines after treatment with OA and UA, respectively. Also, the results of inhibition after exposure to the two compounds incorporated into PU are presented.

One can notice (Figure 6) that OA has a poor cytotoxic activity on the three cancer cell lines at the tested concentrations. Concentration of 10 μM of pure OA inhibited only 2.92 ± 5.39% of the MCF-7 cells while for the T47D human ductal breast epithelial tumor cell line and the MDA-MB-231 human breast carcinoma the inhibition index was 16.11 ± 5.16% and 5.71 ± 2.75%, respectively. Increasing the concentration to 30 μM, an inhibition of 5.98 ± 5.56%, 15.54 ± 6.14% and 11.92 ± 3.44% for the MCF-7, T47D and MDA-MB-231, respectively, was detected. Incorporation of OA inside the PU proved to increase very poorly the inhibition percent on all three cell lines, in both concentrations. Results are as follows: (i) for MCF7 cell line: −1.28 ± 4.55% for 10 μM OA, −8.07 ± 3.28% for 30 μM OA; (ii) for T47D cell line: 7.23 ± 1.28% for 10 μM OA, 20.15 ± 3.24% for 30 μM OA; (iii) for MDA-MB-231 cell line: 10.25 ± 5.56% for 10 μM OA and 17.73 ± 4.95% for 30 μM OA. The polyurethane nanoparticles produced the following inhibition values: (i) for MCF-7 cell line, 3.24 ± 3.47% and −0.74 ± 2.74% for 10 and 30 μM, respectively; (ii) for T47D, 12.56 ± 4.23% and 24.95 ± 3.10% for 10 and 30 μM, respectively; and (iii) for MDA-MB-231 cells, 5.80 ± 1.50% and 13.63 ± 4.30% for 10 and 30 μM, respectively.

In contrast, pure UA (Figure 7) proved to be very active on all three breast cancer lines even at the lowest concentration. Additionally, the PU and UA + PU were also tested on MDA-MD-361 cell lines. For all tested cell lines, the inhibition was more than 90% for both concentrations (10 and 30 μM). Results are as follows: (i) on MCF7 cell line: 93.86 ± 0.72% for 10 μM UA and 93.70 ± 0.46% for 30 μM UA; (ii) on T47D cell line: 95.38 ± 0.79% for 10 μM UA and 95.83 ± 0.78% for 30 μM UA; (iii) on MDA-MB-231 cell line: 95.87 ± 1.04% for 10 μM UA and 95.21 ± 1.11% for 30 μM UA; (iv) on MDA-MB-361 cell line: 91.66 ± 1.82% for 10 μM UA and 91.07 ± 1.70% for 30 μM UA. The growth inhibition results for the UA + PU are as follows: (i) -3.67 ± 2.07%, 22.29 ± 3.73%, 0.48 ± 3.09% and 1.11 ± 6.05% for MCF7, T47D, MDA-MB-231 and MDA-MB-361 cell line, respectively, for the concentration of 10 μM UA and (ii): 2.96 ± 1.45%, 33.58 ± 1.56%, 12.30 ± 4.45%, 11.19 ± 5.61% for MCF7, T47D, MDA-MB-231 and MDA-MB-361 cell line, respectively, for the concentration of 30 μM UA. In order to calculate the IC_{50} values

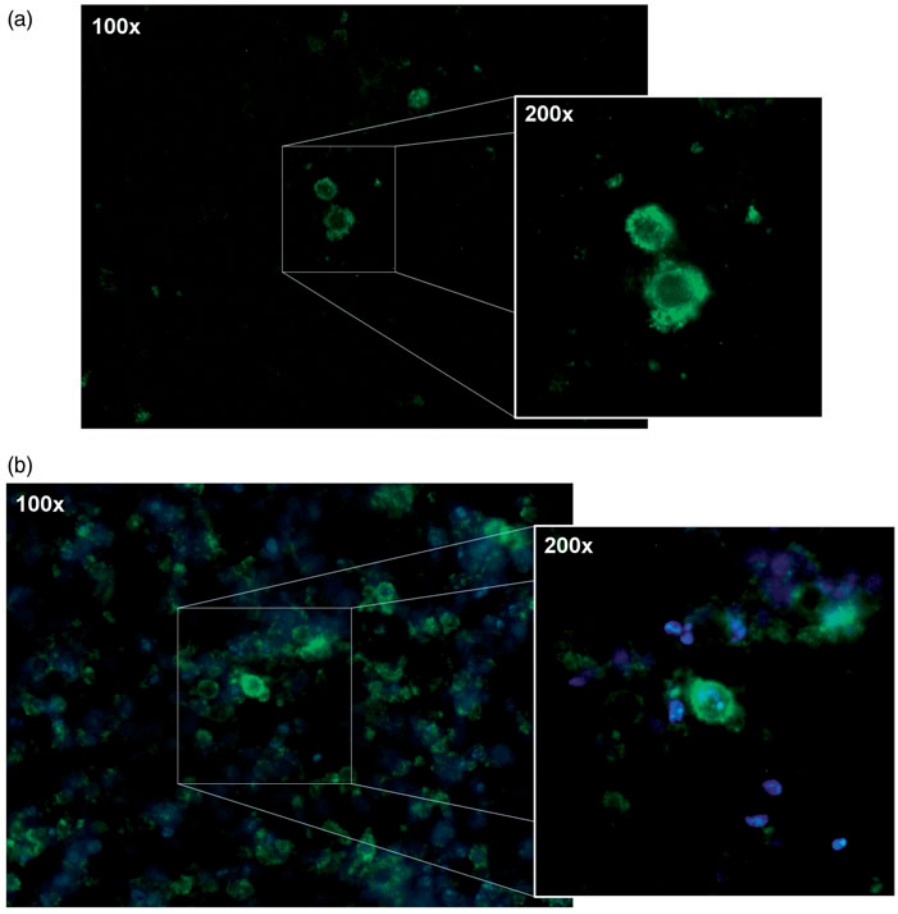

Figure 5. Microscopic images of MCF-7 human breast cancer cells incubated with coumarin-6 loaded nanoparticles after (a) 24 h and (b) 48 h.

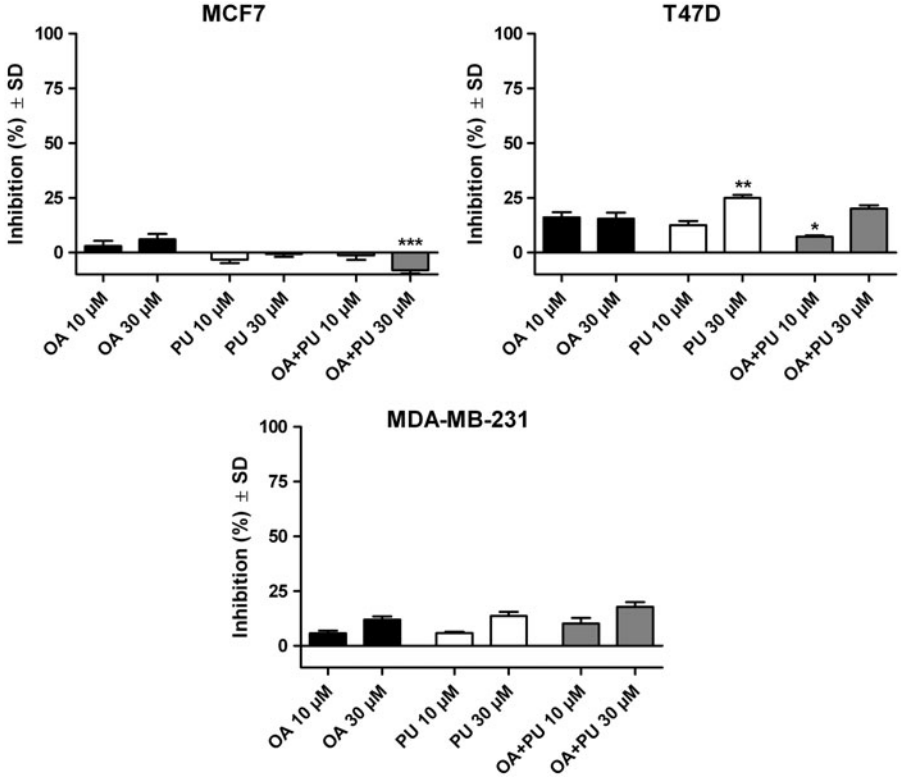

Figure 6. Inhibition of MCF7, T47D and MDA-MB-231 breast cancer cell lines after 72 h exposure on 10 and 30 μM of oleanolic acid (OA), empty polyurethane nanostructures (PU) and polyurethane nanostructures containing oleanolic acid (OA + PU).

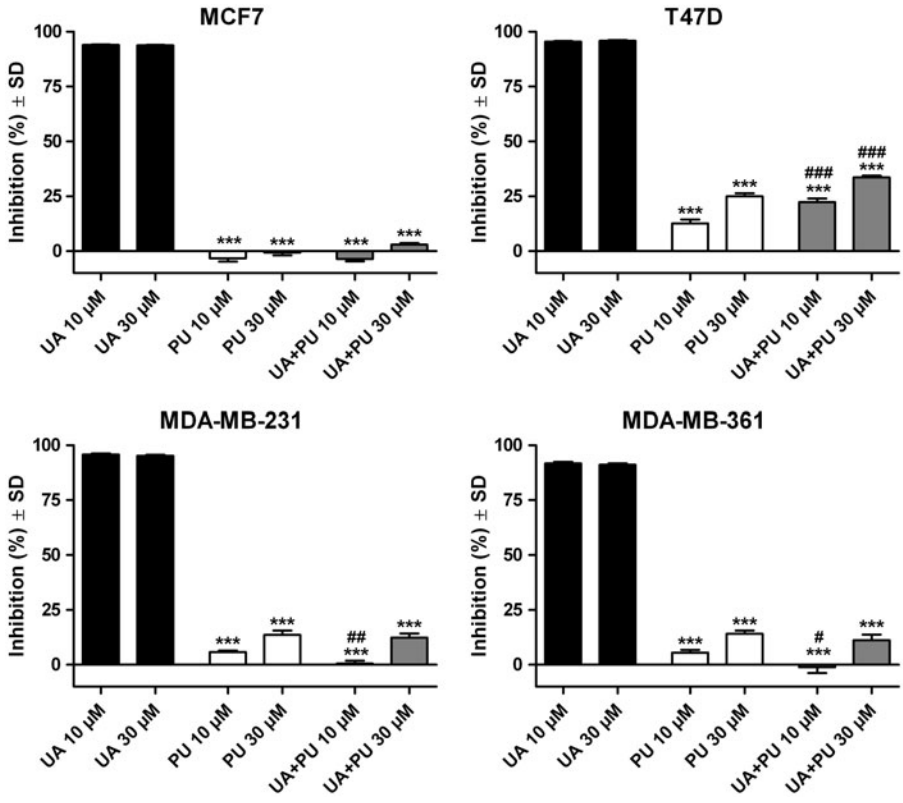

Figure 7. Inhibition of MCF7, T47D and MDA-MB-231 breast cancer cell lines after 72 h exposure on 10 and 30 µM of ursolic acid (UA), empty polyurethane nanostructures (PU) and polyurethane nanostructures containing ursolic acid (UA + PU).

for UA, concentrations between 0.3-10 µM were tested. The calculated IC_{50} values were as follows: 2.47, 1.20, 1.26 and 1.34 µM for MCF7, T47D, MDA-MB-231 and MDA-MB-361, respectively.

In vitro *antibacterial activity*

The *in vitro* antibacterial activity of triterpenic acids and their formulations has been tested on several bacterial strains, Gram-positive and negative, as well as the fungal species, *C. albicans*. OA and UA exhibited antibacterial activity only against *Bacillus cereus* and *Bacillus subtilis* strains. The MIC values were 4570 µg mL^{-1} in case of the *Bacillus cereus,* for both acids, while for *Bacillus subtilis* the MIC values were 2280 and 4570 µg mL^{-1} for OA and UA, respectively. Our study revealed a lack of antimicrobial activity of all samples against the tested strains of Gram-negative bacteria. A loss of *in vitro* antibacterial activity was reported when tested substances were encapsulated into the PUs. Also, both UA and OA showed a poor antifungal activity on *Candida albicans,* with MIC values of 4570 µg mL^{-1}. In terms of antifungal activity when polyurethane nanoparticles were assessed, only those containing oleanolic acid were active against *Candida albicans*.

Discussion

The antitumor potential of the OA and UA is already well known. Researchers have widely studied this activity on different types of cancer, both *in vitro* and *in vivo*. The two compounds have similar chemical structures and therefore similar pharmacological activities, often being studied together (Feng et al. 2009; Chakravarti et al. 2012); also, they are often found together as components of some plants (Feng et al. 2009). However, their antitumor activity is different depending on the cancer cell lines used as well as on potency, in some cases UA proving to be more effective than OA (Liu 1995; Feng et al. 2009).

Chakravarti et al. (2012) studied the anticancer activity of OA and UA as an equimolar mixture extracted from leaves of *Wrightia tomentosa* Roem. & Schult. (Apocynaceae), on MCF-7 and MDA-MB-231 cell lines and concluded that the anti-proliferative effect was due to the induction of apoptosis by extrinsic and intrinsic apoptosis pathways after exposure to the mixture. Shan et al. (2011) reported UA and OA cytotoxic effects against MCF-7/wt cells and adriamycin resistant breast cancer cell line MCF-7/ADR with IC_{50} of 30 and 40 µM UA, respectively. Our study on MCF-7 shows that after 72 h, even small concentrations such as 10 µM UA inhibited more than 90% of the breast cancer cells; similar results were obtained on MDA-MB-231 and T47D cell lines. Shan et al. (2011) also reported cytotoxic effects for OA with IC_{50} values of 28 and 44 µM on MCF-7/wt and MCF-7/ADR, respectively. Contrary to their results, our study reveals that 10 and 30 µM OA failed to inhibit the viability of human breast cancer MCF-7 cells. Moreover, MDA-MB-231 and T47D cell lines appeared to be resistant to the OA treatment. These findings are consistent with other studies that reported a weak cytotoxic activity of OA on both MCF-7 and MDA-MB-231 cells (Hsu et al. 2005; Bishayee et al. 2011). The encapsulation of UA into the PU led to poor *in vitro* results, the growth inhibition significantly decreasing for all cell lines when compared to pure UA. Except for the MCF-7 cell line, the empty polyurethane nanoparticle proved to have an antiproliferative activity of up to 25%. Based on other researchers' results that the association of two compounds with antitumor activity would lead to a synergism of action (Chen et al. 2010; Trandafirescu et al. 2014), we assumed that encapsulation on the active compounds into nanoparticles with own inhibitory activity could result in a potentiation of the inhibitory activity. With respect to the synergistic concept, our

previous studies on ursolic and oleanolic acids formulated as inclusion complexes with cyclodextrins showed a synergistic activity of the active compound and the hydrophilic cyclodextrin which served as a host-molecule for the triterpenic compound (Soica et al. 2014). Contrary to our presuppositions, the encapsulation of ursolic acid into the polyurethane nanoparticles led to poor *in vitro* results, the growth inhibition significantly decreasing for all cell lines when compared to pure ursolic acid. Regarding the encapsulation of oleanolic acid into poliurethane nanoparticles no improvement of *in vitro* anti-proliferative activity was observed.

In terms of antibacterial activity, other studies reported the activity of these pentacyclic triterpenes extracts isolated from medicinal plants. However, many reports are contradictory, other researchers obtaining negative results against the same bacterial strains. Fontanay et al. (2008) reported positive results while using UA and OA against Gram-positive bacteria combined with a lack of activity against Gram-negative bacteria. Although our results confirm the activity of these compounds against *Bacillus subtilis* and *Bacillus cereus*, both Gram-positive bacteria, the MIC values were so high compared with gentamicine (the standard reference against *Bacillus* species, whose MIC is $\leq 0.06\,\mu g\,mL^{-1}$) that the efficacy of the two compounds against the tested strains of *Bacillus* species is questionable. In contrast, do Nascimento et al. (2013) reported UA activity against Gram-negative bacteria. A possible explanation for these contradicting results could be that most studies dealt with antibacterial activity of total plant extracts. After establishing the chemical composition of the extracts, the respective reported activity was attributed to different compounds identified in the extract (Horiuchi et al. 2007). An interesting hypothesis is that the antibacterial activity might be a result of synergism between different herbal components (Fontanay et al. 2008). In terms of triterpenes' activity against *Candida albicans*, antifungal effects were reported by Shai et al. (2008) for UA isolated from *Curtisia dentata* (Burm. F) C.A. Sm. leaves (Cornaceae). As already emphasized, the present paper shows similar antibacterial spectra for both pure UA and OA, but not for the OA + PU and UA + PU, positive results being reported only for OA + PU at a very high concentration.

Based on previous reports that transmembrane transport vehicles could improve the bioavailability of active compounds (Chen et al. 2011; Gao et al. 2012; Zhang et al. 2013), we conducted *in vitro* antitumor and antibacterial tests on PUs containing the two triterpenic acids. Results showed that both active agents were not able to fully exert their pharmacological activity *in vitro* following encapsulation inside PUs. *In vitro* tests are important preliminary tools, providing significant information in terms of biological effects; however, *in vivo* investigations are necessary, given the fact that active substances could be released *in vivo*, following metabolic activity.

Conclusions

Altogether, the paper discusses the *in vitro* anti-proliferative potential of UA on breast cancer cell lines as well as the lack of activity for OA at the same concentrations, in *vitro* antibacterial studies show poor antimicrobial activity of the compounds against *Bacillus* species, a Gram-positive bacterial strain, and antifungal activity against *Candida albicans*, at high doses. Although poor *in vitro* preliminary results are reported for the polyurethane nanoparticles as carriers for the active compounds, *in vivo* evaluations are needed in order to evaluate the possibility of releasing the active compounds as a result of metabolic activity.

Disclosure statement

This paper is partly supported by the UMFT grant PIII-C4-PCFI-2016/2017-03 acronym NANOCEL (to C.O., C.Z., C.S., F.B., V.P., G.T.). Financial support from Bilateral Cooperation in Science and Technology (project numbers: TET_12_RO-1-2013-0033 and UEFISCDI, PN II - Capacities 674/22.04.2013).

References

Bishayee A, Shamima A, Brankov N, Perloff M. 2011. Triterpenoids as potential agents for the chemoprevention and therapy of breast cancer. Front Biosci. 16:980–996.

Bouchemal K, Briançon S, Perrier E, Fessi H, Bonnet I, Zydowicz N. 2004. Synthesis and characterization of polyurethane and poly(ether urethane) nanocapsules using a new technique of interfacial polycondensation combined to spontaneous emulsification. Int J Pharm. 269:89–100.

Chakravarti B, Ranjani M, Siddiqui JA, Bid HK, Rajendran SM, Yadav PP, Konwar R. 2012. *In vitro* anti-breast cancer activity of ethanolic extract of *Wrightia tomentosa*: role of pro-apoptotic effects of oleanolic acid and urosolic acid. J Ethnopharmacol. 142:72–79.

Chen G-Q, Yao Z-W, Zheng W-P, Chen L, Duan H, Shen Y. 2010. Combined antitumor effect of ursolic acid and 5-fluorouracil on human esophageal carcinoma cell Eca-109 *in vitro*. Chin J Cancer Res. 22:62–67.

Chen M, Zhong Z, Tan W, Wan S, Wang Y. 2011. Recent advances in nanoparticle formulation of oleanolic acid. Chin Med. 6:20.

Dehelean CA, Soica C, Peev C, Ciurlea S, Feflea S, Kasa P. 2011. A pharmacotoxicological evaluation of betulinic acid mixed with hydroxipropilgamma cyclodextrin on *in vitro* and *in vivo* models. Farmacia. 59:51–59.

Dehelean CA, Feflea S, Molnar J, Zupko I, Soica C. 2012. Betulin as an antitumor agent tested *in vitro* on A431, HeLa and MCF7, and as an angiogenic Inhibitor *in vivo* in the CAM Assay. Nat Prod Commun. 7:981–985.

Fontanay S, Grare M, Mayer J, Finance C, Duval RE. 2008. Ursolic, oleanolic and betulinic acids: antibacterial spectra and selectivity indexes. J Ethnopharmacol. 2008 120:272–276.

Feng H, Chen W, Zhao Y, Ju X-L. 2009. Anti-tumor activity of oleanolic, ursolic and glycyrrhetinic acid. Open Nat Prod J. 2:48–52.

Gao D, Tang S, Tong Q. 2012. Oleanolic acid liposomes with polyethylene glycol modification: promising antitumor drug delivery. Int J Nanomedicine. 7:3517–3526.

Gayathri R, Kalpana Deepa Prida D, Gunassekaran G, Dhanapal S. 2010. Protective role of ursolic acid in DEN induced oxidative stress mediated hapatocellular carcinoma a focus on thiol status. Int J Pharm Pharm Sci. 2:140–146.

George CV, Kumar NDR, Suresh PK, Kumar RA. 2012. Apoptosis-induced cell death due to oleanolic acid in HaCaT keratinocyte cells-a proof-of-principle approach for chemopreventive drug development. Asian Pac J Cancer Prev. 13:2015–2020.

Horiuchi K, Shiota S, Hatano T, Yoshida T, Juroda T, Tsuchiya T. 2007. Antimicrobial activity of oleanolic acid from *Salvia officinalis* and related compounds on vancomycin-resistant enterococci (VRE). Biol Pharm Bull. 30:1147–1149.

Hsu H-F, Houng J-Y, Chang C-L, Wu CC, Chang FR, Wu YC. 2005. Antioxidant activity, and DNA information of *Glossogyne tenuifolia*. J Agric Food Chem. 3:6117–6125.

Kim S-G, Kim MJ, Jin D, Soon-Nang P, Cho E, Freire MO, Jang S-J, Park Y-J, Kook J-K. 2012. Antimicrobial effect of ursolic acid and oleanolic acid against methicillin-resistant *Staphylococcus aureus*. Kor J Microbiol. 48:212–215.

Kurek A, Nadkowska P, Pliszka S, Wolska KI. 2012. Modulation of antibiotic resistance in bacterial pathogens by oleanolic acid and ursolic acid. Phytomedicine. 19:515–519.

Lopes S, Novais M, Teixeira C, Honorato-Sampaio K, Pereira MT, Ferreira LAM, Braga FC, Oliveira MC. 2013. Preparation, physiochemical characterization, and cell viability evaluation of long-circulating and pH-sensitive liposomes containing ursolic acid. BioMed Res Int. 2013:Article ID 467147. DOI: 10.1155/2013/467147.

Liu L, Wang X. 2007. Improved dissolution of oleanolic acid with ternary solid dispersions. AAPS PharmSciTech. 8:267–271.

Liu J. 1995. Pharmacology of oleanolic acid and ursolic acid. J Ethnopharmacol. 49:57–68.

Mosmann T. 1983. Rapid colorimetric assay for cellular growth and survival: application to proliferation and cytotoxicity assays. J Immunol Methods. 65:55–63.

Mokoka TA, McGaw LJ, Mdee LK, Bagla VP, Iwalewa EO, Eloff N. 2013. Antimicrobial activity and cytotoxicity of triterpenes isolated from leaves of *Maytenus undata* (Celastraceae). BMC Complement Altern Med. 13:111. DOI: 10.1186/1472-6882-13-111.

do Nascimento P, Lemos T, Bizerra A, Arriaga AMC, Ferreira DA, Santiago GMP, Braz-Filho R, Costa JGM. 2013. Antibacterial and antioxidant activities of ursolic acid and derivatives. Molecules. 19:1317–1327.

Prasad S, Yadav VR, Sung B, Reuter S, Kannappan R, Deorukhkar A, Diagaradjane P, Wei C, Baladandayuthapani V, Krishnan S, et al. 2012. Ursolic acid inhibits growth and metastasis of human colorectal cancer in an orthotopic nude mouse model by targeting multiple cell signaling pathways: chemosensitization with capecitabine. Clin Cancer Res. 18:4942–4953.

Rosen H, Abribat T. 2005. The rise and rise of drug delivery. Nat Rev Drug Discov. 4:381–385.

Shai LJ, McGaw LJ, Aderogba MA, Mdee LK, Eloff JN. 2008. Four pentacyclic triterpenoids with antifungal and antibacterial activity from *Curtisia dentata* (Burm. f) C.A. Sm. leaves. J Ethnopharmacol. 119:238–244.

Shan J, Xuan Y, Ruan S, Sun M. 2011. Proliferation-inhibiting and apoptosis-inducing effects of ursolic acid and oleanolic acid on multi-drug resistance cancer cells *in vitro*. Chin J Integr Med. 17:607–611.

Soica C, Dehelean C, Danciu C, Wang HM, Wenz G, Ambrus R, Bojin F, Anghel M. 2012. Betulin complex in γ-cyclodextrin derivatives: properties and antineoplasic activities in *in vitro* and *in vivo* tumor models. Int J Mol Sci. 13:14992–15011.

Soica C, Oprean C, Borcan F, Danciu C, Trandafirescu C, Coricovac D, Crainiceanu Z, Dehelean CA, Munteanu M. 2014. The synergistic biologic activity of oleanolic and ursolic acids in complex with hydroxypropyl-γ-cyclodextrin. Molecules. 19:4924–4940.

Soica C, Danciu C, Savoiu-Balint G, Borcan F, Ambrus R, Zupko I, Bojin F, Coricovac D, Ciurlea S, Avram S, et al. 2014. Betulinic acid in complex with a gamma-cyclodextrin derivative decreases proliferation and *in vivo* tumor development of non-metastatic and metastatic B164A5 cells. Int J Mol Sci. 15:8235–8255.

Sun H, Fang W, Wang W, Hu C. 2006. Structure-activity relationships of oleanane- and ursanetype triterpenoids. Botanical Studies. 47:339–368.

Trandafirescu C, Gheorgheosu D, Borcan F, Oprean C, Ionescu D. 2014. Preliminary evaluation of the synergistic activity of lupeol and betulin. UV Radiation and Skin Pathology, Workshop Timişoara. 18. ISBN 978-606-8456-32-4.

Wang J, Ren T, Xi T. 2012. Ursolic acid induces apoptosis by suppressing the expression of FoxM1 in MCF-7 human breast cancer cells. Med Oncol. 29:10–15.

Workman P. 2001. New drug targets for genomic cancer therapy: successes, limitations, opportunities and future challenges. Curr Cancer Drug Targets. 1:33–47.

Yim EK, Lee MJ, Lee KH, Um SJ, Park JS. 2006. Antiproliferative and antiviral mechanisms of ursolic acid and dexamethasone in cervical carcinoma cell lines. Int J Gynecol Cancer. 16:2023–2031.

Zhang P, Li H, Chen D, Ni J, Kang Y, Wang S. 2007. Oleanolic acid induces apoptosis in human leukemia cells through caspase activation and poly(-adp-ribose) polymerase cleavage. Acta Biochim Biophys Sin (Shanghai). 39:803–809.

Zhang H, Li X, Ding J. 2013. Delivery of ursolic acid (UA) in polymeric nanoparticles effectively promotes the apoptosis of gastric cancer cells through enhanced inhibition of cyclooxygenase 2 (COX-2). Int J Pharm. 441:261–268.